

Intensity pseudo-localized phase in the glassy random laser

Jacopo Niedda^{1,2}, Luca Leuzzi^{2,1,†}, Giacomo Gradenigo^{3,4}

¹ Dipartimento di Fisica, Università di Roma “Sapienza”, Piazzale A. Moro 2, I-00185, Roma, Italy

² NANOTEC CNR, Soft and Living Matter Lab, Roma, Piazzale A. Moro 2, I-00185, Roma, Italy

³ Gran Sasso Science Institute, Viale F. Crispi 7, 67100 L’Aquila, Italy

⁴ INFN-Laboratori Nazionali del Gran Sasso, Via G. Acitelli 22, 67100 Assergi (AQ), Italy

E-mail: † luca.leuzzi@cnr.it

Abstract.

Evidence of an emergent pseudo-localized phase characterizing the low-temperature replica symmetry breaking phase of the complex disordered models for glassy light is provided in the mode-locked random laser model. A pseudo-localized phase corresponds to a state in which the intensity of light modes is neither equipartited among all modes nor strictly condensed on few of them. Such a *hybrid* phase, recently characterized as a finite size effect in other models, such as the Discrete Non-Linear Schrödinger equation, in the low temperature phase of the glassy random laser appears to be robust in the limit of large size.

1. Introduction

The present paper is devoted to the study of a particular phenomenon taking place in quenched disordered models of random lasers [1, 2]: intensity localization of light, else termed *power condensation* [3, 4], and its relationship to the high pumping replica symmetry breaking (RSB) random lasing phase.

It was since the seminal work of Anderson on semiconductors that localization (space localization in this case) has been related to ergodicity breaking [5]. In his most celebrated work Anderson showed that a large enough amount of disorder, in the form of impurities of the alloy, was able to induce the localization in space of the electron wavefunction and the consequent absence of transport, therefore triggering a semiconductor/insulator transition. The insulating-localized phase was clearly characterized by a dynamical breaking of *ergodicity*.

Since the '50s the idea of localization, related to ergodicity breaking, has been conceived also in classical systems: we think of the celebrated Fermi-Pasta-Ulam-Tsingou (FPUT) numerical study on the relaxation from an atypical initial condition in a slightly anharmonic chain. Despite Fermi's expectation that the anharmonicity was sufficient to trigger the fast relaxation of the system to equipartition between the Fourier modes of the chain, an initial condition with only the lowest harmonic excited showed a recurrent dynamics for the whole duration of the numerical experiment, with no signature of relaxation to equipartition [6]. Localization was, thus, coming along with dynamical ergodicity breaking also in the case of energy localization in the Fourier power spectrum.

The paradigm of ergodicity breaking as a dynamical phenomenon manifesting itself as the lack of transport or the absence of relaxation from atypical initial conditions has been the dominant one until the '80s, when a thermodynamic paradigm and a statistical ensembles formalism was established for ergodicity breaking transitions in complex disordered systems: the theory of replica symmetry breaking proposed by Parisi [7, 8]. Quite interestingly, while localization phenomena in quantum many-body systems have been widely investigated during the last decades [9, 10, 11, 12, 13, 14, 15, 16], they have seldom been probed in disordered systems, apart from some attempts, e.g., Refs. [17, 18]. This lack of analysis in disordered glassy systems is due to the nature of the variables which are customary for magnetic disordered systems: Ising, XY or Heisenberg spins are all locally bounded, $|\vec{s}_i| = 1$, $\forall i = 1, \dots, N$, with N being the size of the system. In those models where variables were used with continuous locally unbounded magnitude as a proxy for magnetic spins in spin-glasses or density fluctuations in structural glasses [19, 20, 21, 22, 23, 24], the interaction network was fully connected, thus hindering any sort of magnitude localization. Indeed, this kind of mean-field representation on a complete graph, together with a local potential (soft spins) or a global constraint (spherical spins) guarantees magnitude equipartition.

A careful investigation of how magnitude localization coexists with replica symmetry breaking in disordered systems is therefore a gap that needs to be filled. Some

signatures of strong breaking of intensity equipartition have been already highlighted in Ref. [25] as features of the emission spectra of glassy random lasers at high pumping [26, 27, 28, 29, 30, 31, 32]. By means of numerical simulations on a slightly different model for random lasers with respect to the one of Ref. [25], we will now deepen the study of such phenomenology and we will connect it with the most recent literature on intensity localization in systems with locally unbounded variables and global constraints [17, 18, 33, 34, 35].

The leading model for the non-linear interaction of light modes in a random optically active medium (under external pumping) is the so-called “mode-locked p -spin”, a model with complex spherical spins and mixed p -body potential with both the $p = 2$ and $p = 4$ interactions [?, 25]. The mode-locked p -spin differs from the original fully connected model because not all the possible p -uples of light modes (each mode being identified by his angular frequency ω_k and its complex amplitude $a_k = a(\omega_k)$) participate to the p -body interaction, only those allowed by the symmetries of light-matter interaction in random active media. It is only in the *narrow-bandwidth* approximation that all p -uplets are allowed to interact and contribute to the Hamiltonian. In this case the model has been analytically solved in the framework of Replica Symmetry Breaking theory [2, 36]. In the narrow-bandwidth approximation each light mode interacts with $\mathcal{O}(N^3)$ modes ($p = 4$) and, despite the fact that the continuous variables of the model, i.e. light modes, are locally unbounded, the complete, fully connected, character of the interaction network forbids any sort of inhomogeneous distribution of intensity. Full connectivity enforces intensity equipartition among light modes. On the other hand, in a diluted network the overall magnitude might be subdivided among variables in a non-homogeneous way and, if the dilution is strong enough, magnitude localization might occur.

We stress that power condensation (else termed intensity, or magnitude, localization) is not the generalization to light waves of the spatial wavefunction localization occurring in Anderson theory, that is known to be inhibited in 3D random lasers because of the vectorial nature of light waves [37, 38]. Rather, it is a condensation of the overall magnitude on a few Fourier modes, in presence of a global constraint on intensity. When the value of this globally conserved quantity exceeds a given threshold the system undergoes a transition where a macroscopic fraction of the conserved quantity concentrates, even in the thermodynamic limit, on a finite set of degrees of freedom (Fourier modes in the present case).

As an instance, this behavior has been found and very precisely described in the framework of large deviation calculations and ensemble inequivalence in the case of mass-transport models [39, 40] or for bosonic condensates in optical lattices described by the Discrete Non-Linear Schrödinger Equation (DNLSE) [41]. Concerning the DNLSE, it is known since almost two decades that his high energy phase is characterized by the appearance of localized breather-like solutions, which typically arise in certain regimes in models of non-linear waves [42, 43, 33, 44, 45, 46, 47].

A complete understanding of the relevance of these solutions from the point of view

of equilibrium statistical mechanics has been achieved only recently: in Refs. [17, 18] it has been shown that they are stable equilibrium solutions in the microcanonical ensemble with the peculiarity of having a negative temperature [34, 48, 35, 49, 45]. The presence of a negative temperature, which in the context of the DNLSE comes along with the lack of statistical ensemble equivalence, is a signature of a “thermodynamic anomaly”: the larger the amount of energy fed to the system, the larger the amount of condensate mass localization, hence the smaller the entropy. Such a phenomenon is usually not possible in the canonical ensemble but is perfectly allowed in the microcanonical one.

The very interesting feature of the magnitude localization transition taking place for bosonic condensates on a lattice is the existence of a pseudo-localized phase, which is a sort of precursor of the localized one. This is interesting also in connection to the high pumping behavior of mode-locked random lasers. In the case of the bosonic condensates the pseudo-localized phase is a *hybrid* phase: the participation ratio (the localization order parameter) vanishes for a large number N of degrees of freedom, but it displays a negative temperature, that is a signature of incipient localization. A negative temperature signals a non-standard thermodynamic behaviour, where the entropy decreases by increasing the energy, and a breaking of equivalence between the microcanonical and the canonical ensembles in statistical mechanics. As we are going to discuss, in the high pumping replica symmetry breaking phase of the mode-locked complex spherical p -spin model another hybrid pseudo-localized phase occurs: for large systems the participation ratio goes to zero but the emission intensity spectra are very inhomogeneous.

An important difference between the two cases is that in the DNLSE condensates the pseudo-localization is related to the inequivalence between canonical and microcanonical ensembles, while in the present case it is not. This comes about because in the laser model the hard constraint is not on the energy (as in the microcanonical ensemble) but, rather, on the overall intensity, that does not coincide with the energy. Indeed, in the present work the emergence of a pseudo-localized phase occurs in the canonical ensemble and it can be studied with ordinary (though highly optimized) Monte Carlo algorithms.

We will see that a sensitive order parameter for the pseudo-localization in the mode-locked random laser is related to the spectral entropy signaling the breaking of intensity equipartition occurring at some critical pumping power. This critical point is consistent with the RSB transition point, in the numerical uncertainty of the finite size scaling for the simulated systems. We will show that a fundamental issue in the occurrence of localization or pseudo-localization of intensity in the low temperature/high pumping phase is the connectivity of the nonlinear mode interaction.

2. Model and Objectives

The leading model for the mode-locking random laser is [2, 50, 51, 25]

$$\mathcal{H}[\mathbf{a}] = - \sum_{\mathbf{k}|\text{FMC}(\mathbf{k})} J_{k_1 k_2 k_3 k_4} \bar{a}_{k_1} a_{k_2} \bar{a}_{k_3} a_{k_4} + \text{c.c.}, \quad (1)$$

where the ‘‘spins’’ a_k are the complex amplitudes of the light modes of angular frequency ω_k , satisfying the global ‘‘spherical’’ constraint

$$\sum_k |a_k|^2 = \mathcal{E} = \epsilon N, \quad (2)$$

where $\epsilon = \mathcal{E}/N$ is the optical power per mode available in the system and the quenched disordered couplings $J_{k_1 k_2 k_3 k_4}$ are distributed according to

$$\mathcal{P}(J_{k_1 k_2 k_3 k_4}) = \frac{1}{\sqrt{2\pi\sigma_4^2}} \exp \left\{ -\frac{J_{k_1 k_2 k_3 k_4}^2}{2\sigma_4^2} \right\}, \quad (3)$$

where

$$\sigma_4^2 = \frac{4! J_4^2}{2N^2}. \quad (4)$$

The modes involved in each interaction term must satisfy the frequency matching condition (FMC)

$$\text{FMC}(\mathbf{k}) : |\omega_{k_1} - \omega_{k_2} + \omega_{k_3} - \omega_{k_4}| \lesssim \gamma, \quad (5)$$

where γ is the single mode linewidth. In the simulated system the mode frequencies are chosen according to the simplifying scheme of being ‘‘comb-like’’ distributed,

$$\omega_k = \omega_0 + \delta\omega k, \quad (6)$$

so that the FMC conditions simply read as

$$|k_1 - k_2 + k_3 - k_4| = 0 \quad , k_i = 1, \dots, N. \quad (7)$$

At difference with the model studied in Ref. [25] we impose periodic boundary conditions (PBC) on the mode-frequencies, i. e., given any two mode indices k_a and k_b their distance will be

$$|k_a - k_b| = \begin{cases} |k_a - k_b| & \text{if } |k_a - k_b| \leq \lfloor \frac{N}{2} \rfloor \\ N - |k_a - k_b| & \text{if } |k_a - k_b| \geq \lfloor \frac{N}{2} \rfloor \end{cases}, \quad (8)$$

where $\lfloor N/2 \rfloor$ is the integer part of $N/2$. These conditions on the space of frequencies have been introduced in Ref. [52] to reduce the strong finite-size effects on the numerical results of the ML 4-phaser model dynamics [25]. In practice, band-edge modes participate in the same number of interacting quadruplets as the modes in the center of the spectrum. Therefore, the simulated model at a certain size N can be regarded as

the bulk of the model with free boundaries on the mode frequencies and a size larger than N .

The disorder-dependent partition function is

$$Z_N(\beta, \mathcal{E}) = \int \prod_{k=1}^N da_k d\bar{a}_k e^{-\beta \mathcal{H}[\mathbf{a}]} \delta \left(\mathcal{E} - \sum_{k=1}^N |a_k|^2 \right), \quad (9)$$

where β is proportional to the inverse heat bath temperature. The Hamiltonian (1) is compatible with the “strong-cavity” limit [53], where the 2-body term of the general model mentioned in the introduction can be neglected because of the spherical constraint. This is justified because we are mainly interested in the study of systems near and above the lasing transition, where the nonlinear 4-body term is dominant. We refer to the model (1) as mode-locked (ML) 4-phasor model.

2.1. Connectivity

The variance σ_4^2 of the distribution (3) is of order N^{-2} to guarantee the extensivity of the energy of the thermodynamic states, given by the Hamiltonian (1). In fully connected 4-spin interacting models the variance is of $\mathcal{O}(N^{-3})$, but the condition (5) turns out to dilute the complete graph of interaction of an order N [54]. As already mentioned, it is precisely the dilution introduced by the frequency matching condition that allows for the occurrence of such heterogeneity in the mode intensities to manifest themselves in the form of a pseudo-localized phase arising at the RSB transition.

In appendix Appendix A we go through a scaling argument on generic p -spin interacting systems (both with ordered or disordered interactions) with continuous variables and a global spherical constraint, of which the ML 4-phasor model with the constraint (2) is a special case. In figure (1) we summarize the scaling argument predictions on a pictorial diagram with the known cases of equipartition, localization and pseudo-localization for the 4-spin model. There, on the left side, we include the ordered case, in which the couplings J are not random at all, and the disordered but not frustrated case, in which the J 's are random but their mean square displacement is so small in comparison to the average that frustration does not take place. When frustration dominates, the low temperature/high pumping regime is glassy. This is the case depicted on the right hand side of the figure (1). The present model case has random couplings with zero mean, therefore guaranteeing frustration and glassiness, and an overall connectivity of order N^3 . It is pointed out at by an arrow. To summarize, in a p -spin interacting model, such as the one we are analyzing here, the external parameter driving the transition from an equipartite to a localized regime (passing through a “critical” pseudo-localized phase) is the order of dilution of the mean spin connectivity.

2.2. Hard and soft constraints

The other fundamental ingredient involved in this phenomenology is the spherical constraint (2). In order to understand its role and importance let us draw the parallelism

with other models where localization takes place. Let us consider for instance the DNLSE whose partition function reads

$$\Omega(\mu, E) = \int \prod_{i=1}^N d\psi_i d\bar{\psi}_i e^{-\mu \sum_{i=1}^N |\psi_i|^2} \delta \left(E - \sum_{i=1}^N |\psi_i|^4 \right), \quad (10)$$

where μ is the chemical potential. Clearly the quantity

$$A = \sum_{i=1}^N |\psi_i|^2, \quad (11)$$

represents the mass of the condensate, so that the partition function in Eq. (10) corresponds to an ensemble where exact conservation of energy is enforced by means of a hard constraint whereas mass is conserved only on average by means of a soft constraint.

In the case of the DNLSE, as in *all* cases where it takes place, the physical quantity that localizes is the one controlled by the hard constraint, hence in this case it is the energy. It is only thanks to the *global* action of the constraint on the total energy that configurations with a strongly heterogeneous distribution of energy on lattice sites are allowed. The analytical calculations of Refs. [17, 18] show that as soon as energy is constrained above a certain critical value, $E > E_c$, these localized configurations dominate the partition function. It can be shown analytically, but it is also easy to make sense of it looking at Eq. (10), that one cannot have localization of a quantity controlled “on average”. It is not possible to have strongly inhomogeneous fluctuations

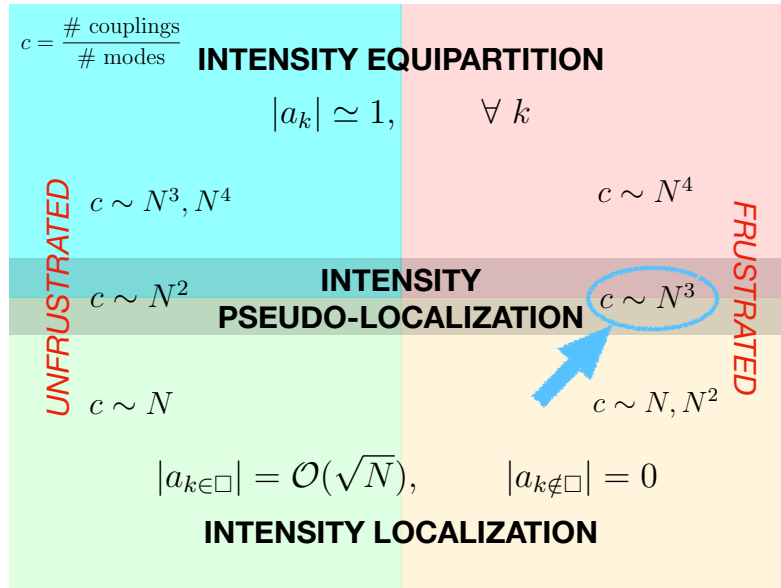


Figure 1. Schematic representation of the possible regimes of low temperature intensity equipartition, intensity localization or pseudo-localization with respect to the coupling dilution in the 4-spin spherical model, both for the unfrustrated version (left) and the frustrated, strongly disordered, one (right). The case of the mode-locked random laser whose connectivity $c \sim N^3$ is pointed at by the arrow.

and/or localization of something which is controlled *homogeneously* by means of a Lagrange multiplier like the chemical potential in Eq. (10). This is precisely the same mechanism of Bose-Einstein condensation, which is a form of localization in Fourier space: the condensed phase can not be reached by controlling density with a chemical potential; density must be tuned directly, for instance decreasing the volume for a given number of bosons [55].

The fact that the Bose-Einstein condensation cannot be implemented by tuning the chemical potential of a reservoir in contact with the system is analogous to the fact that energy localization cannot be achieved by tuning the temperature of a thermostat, i.e. by studying the partition function where conservation of energy is imposed “on average”, as $\exp(-\beta\mathcal{H})$, rather than exactly, as $\delta(E - \mathcal{H})$. In both the above examples localization entails lack of statistical ensemble equivalence: for the energy localization in the DNLSE it is the lack of equivalence between fixed temperature and fixed energy ensembles, for Bose-Einstein condensation it is the lack of equivalence between fixed chemical potential and fixed density ensembles.

What about our random laser? In the partition function of Eq. (9) the conservation of energy is realized on average, by imposing homogeneously a temperature for all interacting quadruplets, while the conservation of the total intensity is realized exactly, by means of the hard global constraint (2). It is then possible to guess that in the ML 4-phaser model the intensity localization might occur, rather than energy. As for the condensation in DNLSE, intensity localization is achieved by tuning the physical quantity \mathcal{E} controlled by the overall hard constraint (2). More precisely, when a certain threshold is overcome in the controlling parameter of the constraint, $\mathcal{E} > \mathcal{E}_c$, configurations where a finite amount of the overall intensity is stored in a few, $\mathcal{O}(1)$, quadruplets might become thermodynamically dominant.

Actually, it is known from the theory [36] that the external parameter driving the phase transition is the pumping rate

$$\mathcal{P} \equiv \frac{\epsilon}{\sqrt{T}}, \quad (12)$$

T being the heat-bath temperature and $\epsilon = \mathcal{E}/N$ being the average intensity per mode defined in Eq. (2). Therefore, \mathcal{P} can be tuned either by varying ϵ at constant temperature (as experiments are usually carried out, apart from some exceptions [56, 57]), or, equivalently, by changing T . In order to numerically simulate the model with Monte Carlo algorithms, one can sample equilibrium configurations at different values of $\beta = 1/T$ from the canonical probability distribution associated to the partition function in Eq. (9) [36, 50, 51]. This is fully equivalent to sample the following probability distribution

$$P[\hat{\mathbf{a}}] \propto e^{-\mathcal{H}[\hat{\mathbf{a}}]} \delta\left(\mathcal{P}N - \sum_{k=1}^N |\hat{a}_k|^2\right), \quad (13)$$

where $\hat{\mathbf{a}}$ denotes rescaled mode amplitude variables $\hat{a}_k \equiv a_k/T^{1/4}$.

So far we have stressed all the formal analogies between the ML 4-phasor model and other models showing localization: continuous locally unbounded variables and the presence of a global constraint. The main difference between the 4-phasor partition function (9) and the partition function (10) of the DNLSE or of the free-bosons, is that in the random laser case the joint distribution of the variables over which the global constraint is imposed is not factorized. Therefore, the analytical results discussed in [17, 18] cannot be straightforwardly extended to this case. Nevertheless, those systems share a feature that turns out to be crucial also for the present model: the existence of an anomalous “pseudo-localized” phase. In the non-interacting systems the anomaly is accompanied by a negative temperature, that is, by a lack of the canonical-microcanonical ensembles equivalence. The anomalous phase shows some signatures of incipient localization but it is not a localized phase. As we are going to show, these are the signatures that we find also in the ML 4-phasor model, by means of Monte Carlo numerical simulations above the pumping rate threshold \mathcal{P}_c (that is proportional to the intensity threshold ϵ_c at fixed temperature) or, equivalently, below the critical temperature T_c , keeping the spherical constraint fixed ($\epsilon = 1$).

3. Pseudo-localization

First of all let us provide a qualitative information about the behaviour of the spectrum when T is lowered, which can be read off equivalently as an increase of the spherical constraint value: see Eq. (13). In Fig. 2 the time-average of the spectrum at equilibrium is shown for different values of the temperature and a single instance of the quenched disorder (a single realization of the couplings J). It can be very clearly seen that, as the pumping is increased (temperature is decreased) the overall intensity tends to be heterogeneously distributed among the modes. This might hint that a localization phenomenon in intensity occurs but it is not enough to establish it. Whether the system truly localizes or not can be ascertained only from the study of the localization order parameter, the participation ratio:

$$Y_2 = \left\langle \frac{\sum_{k=1}^N I_k^2}{\left(\sum_{k=1}^N I_k\right)^2} \right\rangle = \frac{1}{N^2} \left\langle \sum_{k=1}^N I_k^2 \right\rangle, \quad (14)$$

where $I_k = |a_k|^2$ and we have used that

$$\sum_{k=1}^N I_k = N \quad (15)$$

because of equation (2), with $\epsilon = 1$. The dependence on the number of degrees of freedom of Y_2 can be easily rationalized in two extreme situations: equipartition and localization of the mode intensity. Let us consider localization first: in this case a finite fraction of the whole intensity is taken by a finite number of modes that does not increase

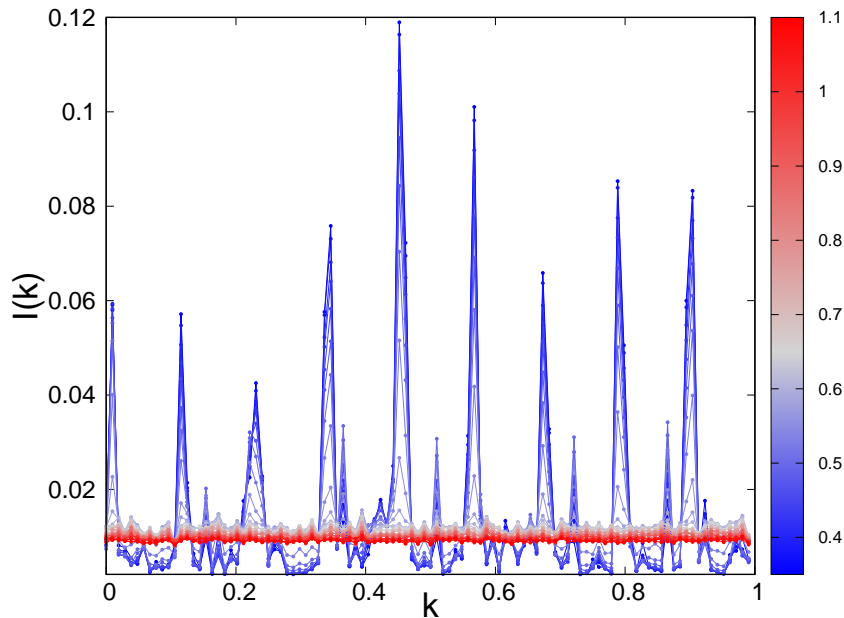


Figure 2. Intensity spectra $I(k) = |a_k|^2/T$ for varying optical pumping rate $\mathcal{P} = 1/\sqrt{T}$ ($\epsilon = 1$), see Eq. (12), as a function of the mode index k for a single realization of quenched disorder of the ML 4-phasor model with PBC on the frequencies. Numerical simulations of size $N = 104$. The spectra are normalized and the modes k are divided by N . Color map: temperature T increases (optical power decreases) from blue to red. Notice the absence of the spectrum curvature, due to PBC on the FMC, and the presence of the isolated peaks below $T_c \simeq 0.61$.

with N , see Appendix Appendix A. That is, in the localized phase, a few modes k have intensity

$$I_k \propto N, \quad (16)$$

whereas all the others $I_{\neq k} = 0$. Then, we have

$$\sum_{k=1}^N I_k^2 \simeq \sum_{k=1}^{\#\text{loc modes}} I_k^2 \propto N^2.$$

This implies that in a localized phase the participation ratio Y_2 in the limit $N \rightarrow \infty$ is a constant that does not depend on N :

$$\text{localization} \iff \lim_{N \rightarrow \infty} Y_2 = \text{const.} \quad (17)$$

On the contrary, in the equipartite phase of nearly homogeneous spectral intensities, any of the N modes has intensity $I_k = \mathcal{O}(1)$, so that in the thermodynamic limit

$$\text{equipartition} \iff Y_2 \sim \frac{1}{N}. \quad (18)$$

Now we are ready to display, in Fig. 3, the first important quantitative information obtained from the study of the equilibrium distribution of the intensity among modes. In the figure we have plotted for convenience the average over quenched disorder of

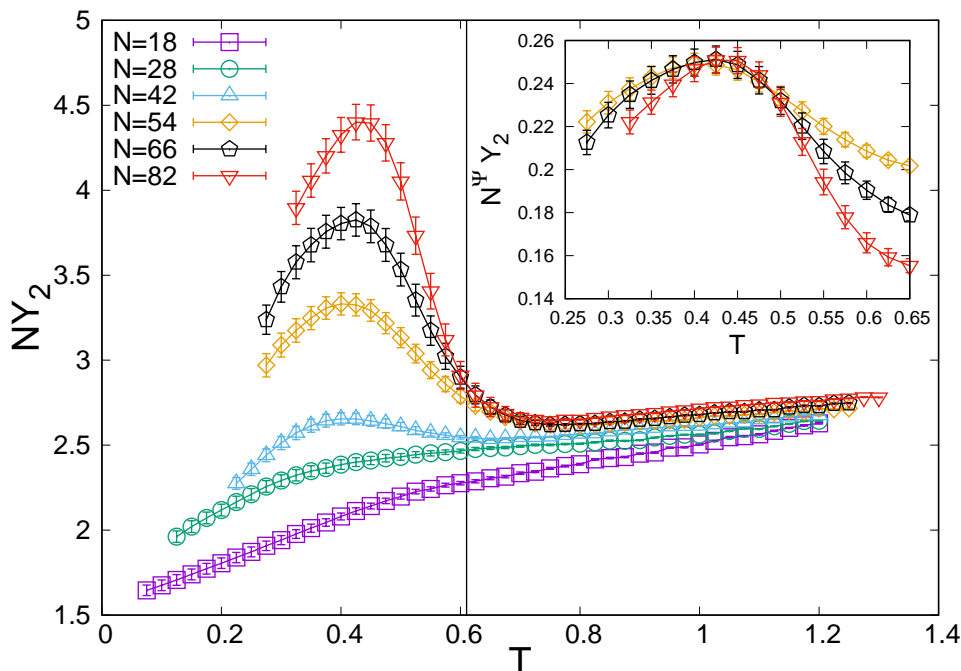


Figure 3. Main: Participation ratio NY_2 of the mode intensities versus T at different systems sizes N . The vertical line is the asymptotic value of the critical temperature for the system $T_c \simeq 0.61$ (from [52]). Inset: scaling of the participation ratio near the peak for the three largest sizes, as $N^\Psi Y_2$ versus T , with $\Psi = 0.35 > 0$. The peak height scaling is less than N , thus Eq. (14) tends to zero as $N \rightarrow \infty$.

$NY_2(T)$, which we expect of $\mathcal{O}(1)$ in the equipartite phase and of $\mathcal{O}(N)$ in a possible localized phase. We observe that in the high temperature phase $NY_2 \sim \text{const}$ and, therefore, the system is in the equipartition regime. Under the critical point, indicated by the vertical line at $T_c = 0.61$, which is the glass transition temperature for this specific model extrapolated in the thermodynamic limit (see [52]), we find, instead, a departure from equipartition. Such behaviour is evident in the whole low T region probed by our numerical simulations. Yet, $NY_2(T)$ does not display an extensive scaling with N , as one would expect for the localized regime according to Eqs. (14,17). In the main panel of Fig. 3, by collapsing the curves around $T = 0.42$, where the peaks of $NY_2(T)$ occur, we observe that $NY_2(T)$ grows with N less than linearly. In this specific case we find $Y_2(T) \sim N^{-\Psi}$ with $\Psi \simeq 0.35$. This is the slowest scaling obtained from our data. As lower T regions are considered for the scaling with N the Ψ exponent slightly increases in the range of simulated temperatures and sizes (it is $\Psi \simeq 0.5$ at the lowest simulated temperatures). We, thus, find no evidence for the low T regime to show intensity condensation, though it is not equipartite either.

The difference from the localization scaling in N , cf. Eq. (17), i.e. $\Psi = 0$, cannot be accounted for as a finite size effect, as it is usually hypothesized in the estimate of critical exponents of a second order phase transition. The latter effects are, indeed, due to the cutting of long-wavelength fluctuations in a finite size lattice. Localization is, instead, controlled by a first-order mechanism where a finite fraction of the whole

localizing quantity concentrates on a few variables in such a way that Y_2 is strictly independent from N . In the glassy phase we, thus, have a phase that might show some signature of incipient localization but it is certainly not localized in intensity. Intensity equipartition is broken but no finite group of modes takes all the intensity of the system. A scaling argument for the onset of such phenomenon is reported in Sec. 2.1 and Appendix Appendix A.

The existence of a similar pseudo-localized phase has been predicted for the DNLSE [17, 18]. The peculiarity of the localization phenomenon in that case is that it takes place in two steps. By increasing the energy, i.e. the quantity controlling localization, one first encounters a second order transition at a value of the energy – E_{th} – where the equivalence of ensembles breaks down and temperature becomes negative. Then, at a larger value of energy, $E_c > E_{th}$, there is a first-order transition to a localized phase. As we mentioned already in the random laser case the quantity controlling localization is the overall light mode intensity, and not the energy, so that we cannot identify the transition to the pseudo-localized phase with a negative temperature and the breaking of equivalence between canonical and microcanonical ensembles.

What can signal the onset of a non-trivial pseudo-localized phase in the ML 4-phaser model? A straightforward answer is to look for an indicator of equipartition, like the spectral entropy or the related effective fraction of degrees of freedom [58, 59].

The spectral entropy is defined as

$$S_{sp} = - \sum_{k=1}^N \hat{\mathcal{I}}_k \ln(\hat{\mathcal{I}}_k), \quad (19)$$

where $\hat{\mathcal{I}}_k$ is the thermal averaged intensity of the mode k normalized to the total intensity of the spectrum

$$\hat{\mathcal{I}}_k = \frac{\langle I_k \rangle}{\sum_{k=1}^N \langle I_k \rangle} = \frac{\langle |a_k|^2 \rangle}{N\epsilon}. \quad (20)$$

The effective fraction of degrees of freedom, which is a function of the spectral entropy and allows to better visualize the information encoded in the spectral entropy, is defined as

$$n_{\text{eff}} = \frac{e^{S_{sp}}}{N}.$$

The behaviour of n_{eff} , averaged over quenched disorder, is reported in Fig. 4 and shows the signature of a phase transition, where equipartition breaks down, at a temperature compatible with the critical transition temperature of the glassy random laser with frequency periodic boundary condition. Its behavior turns out to be qualitatively similar to the one of the effective fraction of degrees of freedom for the model with free boundary conditions on the frequencies analyzed in Ref. [25]. The same analysis with further indicators shows that this equipartition-breaking transition is of first order in the parameter n_{eff} .

In Fig. 4 we notice that in the high temperature phase all the curves approach one, while they decrease to a size-dependent quantity for low temperature: the larger

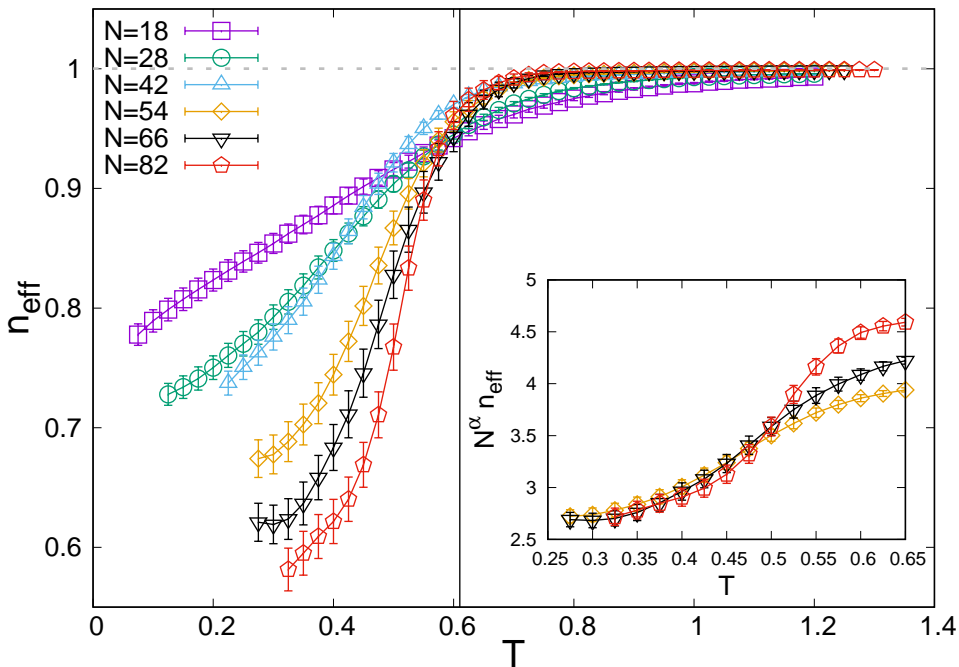


Figure 4. Main: Effective number of degrees of freedom n_{eff} versus T for the mode intensities $|a_k|^2$ for different systems sizes. The vertical line denotes the critical temperature for the system, $T_c \simeq 0.61$. Inset: $N^\alpha n_{\text{eff}}$ versus T , $\alpha = 0.33$.

the size, the steeper n_{eff} decreases. In the inset, we plot the rescaled effective fraction of degrees of freedom for the three largest sizes. In the low temperature phase they collapse on each other with an exponent $\alpha \simeq 1/3$. Thus, in the thermodynamic limit, n_{eff} tends to 0 below the RSB critical point, marking the breaking of equipartition.

The transition taking place at T_c , besides being a glass transition, can, thus, be characterized as the transition to a phase with a thermodynamic anomaly, the breakdown of equipartition, in an analogous way for which we have a breakdown of ensemble equivalence in a non-interacting system such as the DNLSE.

The analogy with the DNLSE holds also for what concerns the spectral intensity distributions, cf. Figs. 5, 6. We can observe in Fig. 5 that, as temperature is lowered, the occurrence of the anomalous phase with lack of equipartition is signaled by the onset of fat tails of the quenched average distribution $P(|a|^2)$. By looking at the distributions for single instances of the random couplings J , see Fig. 6, one can understand that the tails in the average distribution come about because of the occurrence of a secondary peak at large intensity, which, in a hypothetical strictly condensate phase, would become the typical “condensate bump”. This peak also appears in the marginal distribution of energy in the DNLSE (see Fig. 5 in [17]). In that case, though, the non-monotonic behavior of the marginal intensity distribution eventually signals the approach to a truly localized phase.

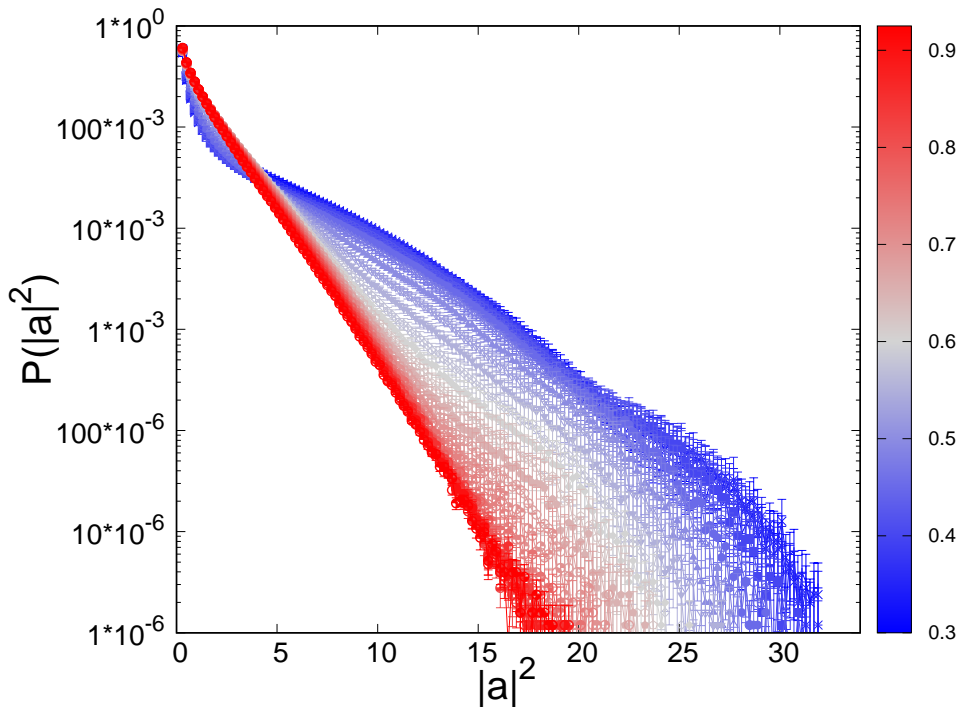


Figure 5. Marginal distribution of spectral intensity averaged over quenched disorder for the system size $N = 82$ at all the simulated temperatures. Color map: as in Fig. 2. At high temperature the distribution is exponentially decaying as revealed by the linear trend in semilogarithmic scale (red curves). By lowering the temperature deviation from monotonicity can be observed (blue curves) in relation to the onset of the pseudo-localized phase.

4. Conclusions

In this work we have presented a detailed analysis of which signatures of intensity localization in light modes spectrum are emerging in the glassy phase of light when the interaction between modes is represented by the so-called “mode-locked” p -spin model with periodic boundary condition on the mode frequencies. This model offers a unique benchmark to study the coexistence between localization and phase-space fragmentation, thanks to its peculiarity with respect to the most commonly studied models of disordered systems: it has continuous, locally unbound, variables with non-linear diluted interactions. These are diluted enough to allow for relevant intensity heterogeneities at low T , cf. Fig 2.

From a careful finite-size study of the participation ratio of the mode intensities we have been able to assess that, although some signatures of *incipient* localization can be found, the glassy phase of light is not, strictly speaking, localized in intensity. This means that the results of our analysis are not compatible with single light modes carrying an extensive amount of intensity, i.e. there is no k such that $|a_k|^2 \sim N$. We have found an anomaly in the finite-size study of the participation ratio, whose size dependence is compatible with the presence of high power modes, carrying an intensity

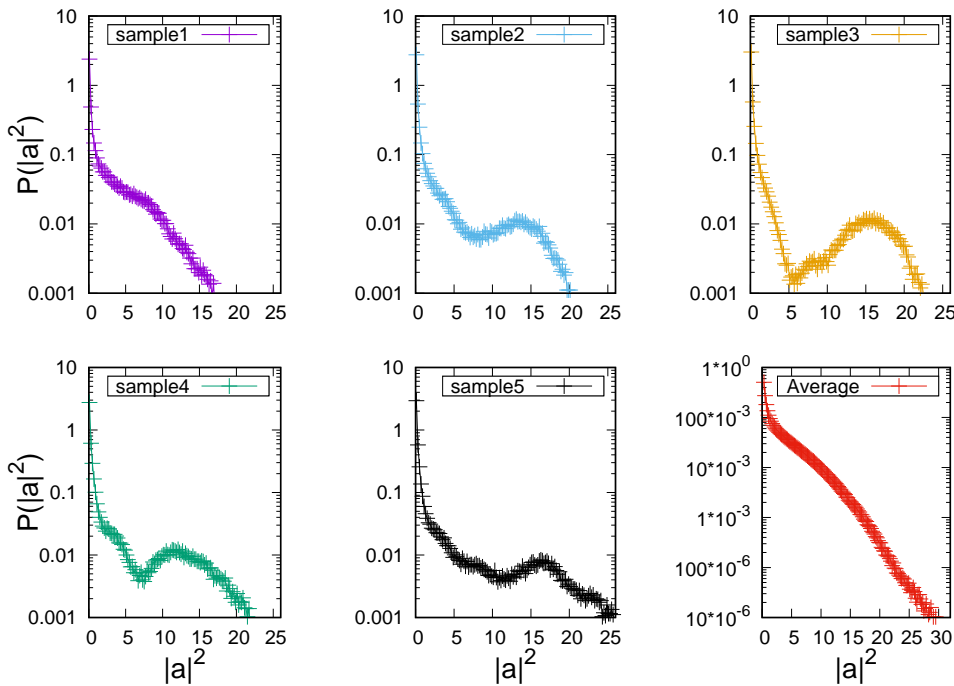


Figure 6. Marginal intensity distributions for single instances of the quenched disorder. Data are referred to the simulated size $N = 82$ at the temperature $T = 0.3$. We notice that some of the samples (such as sample 2,3,4 and 5) exhibit a peak for large mode intensity of the distribution, corresponding to accumulation of the intensity on a few modes. The position of the peak is sample dependent. On the other hand, other samples behave as sample 1, exhibiting only thick tails in the marginal intensity distribution. The result of averaging over all the disordered samples is reported in the sixth panel, which corresponds to the lowest temperature intensity distribution in Fig. 5.

$|a_k|^2 \sim N^{1-\Psi/2}$, with $\Psi > 0$. We stress that in presence of power condensation those modes would have intensity $|a_k|^2 \sim N$, cf. Eq. (17), i.e., $\Psi = 0$. We have termed this phase “pseudo-localized” phase.

In recent literature [17, 18], a similar phase has been discovered and characterized from the theoretical point of view in a simpler non-interacting model, the discrete non-linear Schrödinger equation (DNLSE). In both models the pseudo-localized phase is characterized by a non-monotonic shape of the marginal probability distribution of the quantity under probe, i.e., the site energy for the DNLSE and the overall intensity of light modes for the mode-locked p -phasor model. Due to the different nature of the global constraint controlling the localization and to the presence of mode interactions in the random laser model, though, the mechanisms leading to the pseudo-localized phase differ. The DNLSE is characterized by negative temperature, whereas the pseudo-localized phase of the mode-locked random laser model is characterized by the breaking of equipartition, which can be observed very clearly in emission spectra upon increasing the pumping rate both in numerical simulations and experiments on random lasers [60]. The parameter driving the localization transition in the DNLSE is the energy, while in

the random laser power it appears to be the dilution of the interaction network.

In conclusion, we have presented a comprehensive study of light intensity localization (on Fourier modes), also known as *power condensation* [3, 4], in a disordered model for glassy light, the mode-locked random laser with periodic boundary condition on the frequencies [52]. There are still many open questions and problems to be addressed: in the first place, to achieve an analytic control of the localization phenomenon in non-trivial disordered interacting models like the mode-locked p -phasor model; second, by means of a consistent theoretical modelling of the phenomenon, to gather a precise quantitative control of the dilution needed to allow the appearance of a truly localized phase in the model.

5. Acknowledgements

We thank Daniele Ancora, Maria Chiara Angelini, Roberto Livi, Giorgio Parisi and Federico Ricci Tersenghi for useful discussions. We acknowledge the support of LazioInnova - Regione Lazio under the program Gruppi di ricerca 2020 - POR FESR Lazio 2014-2020, Project NanoProbe (Application code A0375-2020-36761).

Appendix A. Intensity equipartition vs localization and the interaction network connectivity

Let us consider a generic p -spin interacting model with N continuous spins σ and a spherical constraint

$$\sum_{i=1}^N \sigma_i^2 = N, \quad (\text{A.1})$$

whose Hamiltonian is

$$\mathcal{H}[\sigma] = - \sum_{k_1 \dots k_p}^{\#N^A} \sigma_{k_1} \dots \sigma_{k_p} J_{k_1 \dots k_p}, \quad (\text{A.2})$$

where N^A on top of the sum, with $A \in [1, p]$, denotes the scaling with the size of the number of p -uples contributing to the energy and the spin indices k_i run from 1 to N . If $A = p$ we have a fully connected interaction graph, i.e., each spin contributes in $\mathcal{O}(N^{p-1})$ p -uples. On the other extreme, if $A = 1$ the graph is *sparse*, i.e. each spin only interacts in a finite number of p -uples, not growing with the size of the system. All dilutions in between will be considered hereafter.

For simplicity, we will take the variables as real valued here, yet keeping the word *intensity* for the spin magnitude $|\sigma|$.

We notice that the glassy random laser is a model belonging to this family, with $p = 4$ but with complex spins. Though complex variables yield some new physical features we stress that these are not relevant for what concerns the influence of connectivity on the possible onset of intensity localization.

First we consider the ordered case $J_{k_1\dots k_p} = J$. The typical ground state spin configurations in the canonical ensemble, where equipartition is expected to hold (in the average, not strictly), are those minimizing Eq. (A.2). The energy is extensive

$$E = \mathcal{H}[\sigma_{\text{gs}}] = \mathcal{O}(N)$$

provided that the coupling constant scales as

$$J \propto \frac{1}{N^{A-1}}. \quad (\text{A.3})$$

If intensity localization occurs, that is, if only a few modes take the overall intensity, equal to N according to Eq. (A.1), whereas all the other are zero, what will be the energy contribution of a localized spin configuration? First of all let us notice that in order to have a non-zero contribution the intensity of at least p coupled spins must localize. If we represent by \square such a localizing p -uple the intensity localized configuration is

$$\{\sigma_{\text{loc}}\} : \quad \sigma \in \square \propto \sqrt{N} \quad , \quad \sigma \notin \square = 0. \quad (\text{A.4})$$

According to Eqs. (A.2), (A.3) the energy of such a configuration of spins scales with N like

$$E_{\text{loc}} = \mathcal{H}[\sigma_{\text{loc}}] = \mathcal{O}\left(\frac{N^{p/2}}{N^{A-1}}\right).$$

To figure out whether intensity condensation might occur and dominate, one eventually has to compare the scaling behaviors of the energies of an equipartite and a localized configuration:

$$\mathcal{O}(N) \quad \text{vs} \quad \mathcal{O}(N^{\frac{p}{2}+1-A}).$$

The following cases occur depending on the interaction connectivity scaling N^A :

- (i) $A > p/2$. Any possible intensity localized configuration of spins would yield subextensive contributions to the energy. The equipartite regime is, therefore, dominant. The case $A = p$ is the fully connected interaction graph.
- (ii) $A = p/2$. Both kinds of spin configurations yield an $\mathcal{O}(N)$ contribution to the energy. In this case a pseudo-localized phase might occur.
- (iii) $A < p/2$. Intensity localization provides the most prominent contribution to the energy, that is, $\mathcal{O}(N^{>1})$. The case $A = 1$ is the sparse case.

If the interaction couplings $J_{k_1\dots k_p}$ are quenched disordered, independently distributed and with zero mean $\overline{J_{k_1\dots k_p}} = 0$, the typical ground state of the Hamiltonian (A.2) is extensive – $E = \mathcal{H}[\sigma_{\text{gs}}] = \mathcal{O}(N)$ – if the variance of the distribution of the couplings scales like

$$\overline{J_{k_1\dots k_p}^2} \propto \frac{1}{N^{A-1}}. \quad (\text{A.5})$$

If the total intensity of the system is localized in a single interacting p -uple, as in (A.4), Eqs. (A.2), (A.5) imply that the energy scales with the size like

$$E_{\text{loc}} = \mathcal{H}[\sigma_{\text{loc}}] = \mathcal{O}\left(\frac{N^{p/2}}{N^{(A-1)/2}}\right).$$

N	N_4	T_{\min}	T_{\max}	N_{PT}	N_{MCS}	N_s
18	2^9	0.05	1.2	46	2^{19}	200
28	2^{11}	0.1	1.2	44	2^{19}	200
42	2^{13}	0.2	1.2	40	2^{20}	150
54	2^{14}	0.25	1.25	40	2^{20}	100
66	2^{15}	0.25	1.25	40	2^{20}	100
82	2^{16}	0.3	1.3	40	2^{20}	100
104	2^{17}	0.35	1.3	38	2^{21}	80

Table B1. Details for the numerical simulations of the ML 4-phaser model with PBC on the frequencies.

Comparing the equipartite contribution $E = \mathcal{O}(N)$ and the localized contribution E_{loc} we find the following three regimes as the exponent A varies:

- (i) $A = p$. Localized energy contributions are subextensive. The equipartite regime is dominant. This is the fully connected interaction graph case.
- (ii) $A = p - 1$. Both kinds of spin configurations yield an $\mathcal{O}(N)$ contribution to the energy. This is the case, e.g., of the mode-locked glassy random laser, studied in the present work, where $p = 4$, $A = 3$. In this case one might conjecture the occurrence of a pseudo-localized phase.
- (iii) $A < p - 1$. Intensity localization provides superextensive contributions to the energy.

Appendix B. Monte Carlo simulation algorithm on GPU's

The numerical simulations of the ML 4-phaser model have been performed by means of a Parallel Tempering Monte Carlo algorithm [61] parallelized on GPU's. All the details about the algorithm can be found in [25, 52]. Here, we just sketch its most important features and report the details of the simulations, for the reader's convenience.

Given a system size N , for each sample of disorder, the Mode-Locked graph of the interactions is generated, by applying the Frequency Matching Condition with frequency Periodic Boundary Condition to a generated fully-connected graph with $N(N-1)(N-2)(N-3)/24$ quadruplets. Each one of these, if satisfying the FMC, is progressively added to the ML graph up to a preassigned number N_4 : the power of 2 nearer to the total number of quadruplets satisfying the FMC at the given simulated size.

The numerical values of the interacting quadruplets $\{J_{\mathbf{k}}\}$ are independently extracted from the Gaussian distribution Eq. (3). The Metropolis dynamics of NPT replicas of the system at different temperatures is run in parallel on GPU's with the Parallel Tempering algorithm. The temperatures are chosen in order to have almost one third of the replicas below the critical temperature and two thirds above and have an

exchange rate between thermal baths at nearby temperatures staying constant for all temperature couples.

A subtle point of our algorithm is that each update of the dynamics must be compatible with the spherical constraint $\sum_k |a_k|^2 = \epsilon N$. Given the non-locality of this constraint on the configurations, variables updates must be done sequentially. Given two randomly chosen variables $a_i = A_i e^{i\phi_i}$ and $a_j = A_j e^{i\phi_j}$, the local attempt is based on the extraction of three random numbers $x, y \in [0, 2\pi]$ and $z \in [0, \pi/2]$: the first two correspond to the new (attempted) phases $x = \phi'_i$ and $y = \phi'_j$, the third one mixes the intensities of the modes selected by preserving the spherical constraint, since $A'_j = \sqrt{A_i^2 + A_j^2} \cos z$ and $A'_i = \sqrt{A_i^2 + A_j^2} \sin z$. The computation of the energy shift between the original configuration and the attempted one ($a_\ell \rightarrow a'_\ell$) requires a number of operations scaling with the number of quadruplets involved in the variation of a_ℓ

$$\begin{aligned} \Delta E_\ell &= (a_\ell - a'_\ell) \sum_{k_1, k_2, k_3}^{\text{FMC}(k_1, k_2, k_3, \ell)} J_{k_1 k_2 k_3 \ell} \bar{a}_{k_1} a_{k_2} \bar{a}_{k_3} + \text{c.c.} \\ &= \mathcal{O}(N^2). \end{aligned}$$

This computation has been parallelized on GPU's, to speed up the algorithmic time and perform the above average in $\mathcal{O}(\ln N)$ steps. Moreover, also the Parallel Tempering dynamics at different temperatures has been parallelized on GPU's. The two kinds of parallelization considered together reduce the execution time of the entire simulation by a factor of 8.

Exchanges among configurations of replicas at adjacent temperatures are proposed after a fixed number of steps of the local Metropolis algorithm and accepted with a probability that depends on the Boltzmann weights of the replicas involved in the exchange. This helps to speed up the relaxation dynamics of the low temperature replicas of the system, which move in a complex rugged free-energy landscape. We rigorously ascertained the thermalization of each sample by looking at the relaxation of energies on logarithmic time windows and by checking the symmetry of the Parisi overlap distribution function, the order parameter of the glass transition [8].

Once thermalization is tested and an equilibrium time τ_{eq} is estimated, we sampled $\mathcal{N} = (N_{\text{MC}} - \tau_{eq})/\tau_{\text{corr}}$ equilibrium configurations, where N_{MC} is the total number of Monte Carlo steps chosen large enough to have a good statistics and τ_{corr} is the auto-correlation time of mode amplitudes, that we consider in order to not underestimate statistical errors. Canonical ensemble averages over observables are computed through the time average over uncorrelated equilibrium configurations \mathbf{a}_t

$$\langle O[\mathbf{a}] \rangle = \frac{1}{\mathcal{N}} \sum_{t=\tau_{eq}/\tau_{\text{corr}}}^{N_{\text{MC}}/\tau_{\text{corr}}} O[\mathbf{a}_t]. \quad (\text{B.1})$$

All details of the simulations are reported in Table B1.

- [1] Angelani L, Conti C, Ruocco G and Zamponi F 2006 *Phys. Rev. Lett.* **96** 065702
- [2] Antenucci F, Conti C, Crisanti A and Leuzzi L 2015 *Phys. Rev. Lett.* **114** 043901

- [3] Antenucci F, Ibáñez Berganza M and Leuzzi L 2015 *Phys. Rev. A* **91**(4) 043811
- [4] Antenucci F, Ibáñez Berganza M and Leuzzi L 2015 *Phys. Rev. B* **92** 014204
- [5] Anderson P 1958 *Phys. Rev.* **109** 1492
- [6] Fermi E, Pasta J and Ulam S M 1955 *LANL Report*. **1940**
- [7] Parisi G 1979 *Phys. Rev. Lett.* **43** 1754–1756
- [8] Mézard M, Parisi G and Virasoro M 1987 *Spin Glass Theory and Beyond* (World Scientific (Singapore))
- [9] Altshuler B L, Gefen Y, Kamenev A and Levitov L S 1997 *Phys. Rev. Lett.* **78**(14) 2803–2806
- [10] Basko D, Aleiner I and Altshuler B 2006 *Annals of Physics* **321** 1126–1205 ISSN 0003-4916
- [11] Nandkishore R and Huse D A 2015 *Annual Review of Condensed Matter Physics* **6** 15–38
- [12] Ros V, Müller M and Scardicchio A 2015 *Nuclear Physics B* **891** 420–465 ISSN 0550-3213
- [13] Vidmar L and Rigol M 2016 *Journal of Statistical Mechanics: Theory and Experiment* **2016** 064007
- [14] Abanin D A and Papi Z 2017 *Annalen der Physik* **529** 1700169
- [15] Alet F and Laflorencie N 2018 *Comptes Rendus Physique* **19** 498–525 ISSN 1631-0705
- [16] Mossi G and Scardicchio A 2018 *Phil. Trans. R. Soc. A* **375** 20160424
- [17] Gradenigo G, Iubini S, Livi R and Majumdar S N 2021 *Journal of Statistical Mechanics: Theory and Experiment* **2021** 023201
- [18] Gradenigo G, Iubini S, Livi R and Majumdar S N 2021 *Eur. Phys. J. E* **44** 29
- [19] Kirkpatrick T R and Thirumalai D 1987 *Phys. Rev. B* **36** 5388–5397
- [20] Kirkpatrick T R, Thirumalai D and Wolynes P G 1989 *Phys. Rev. A* **40** 1045
- [21] Crisanti A and Sommers H 1992 *Z. Phys. B* **87** 341
- [22] Crisanti A, Leuzzi L and Paoluzzi M 2011 *Eur. Phys. J. E* **34** 98
- [23] Sun Y, Crisanti A, Krzakala F, Leuzzi L and Zdeborová L 2012 *Journal of Statistical Mechanics: Theory and Experiment* **2012** P07002
- [24] Crisanti A and Leuzzi L 2013 *Nucl. Phys. B* **870** 176–204
- [25] Gradenigo G, Antenucci F and Leuzzi L 2020 *Phys. Rev. Research* **2**(2) 023399
- [26] Folli V, Puglisi A, Leuzzi L and Conti C 2012 *Phys. Rev. Lett.* **108** 248002
- [27] Folli V, Ghofraniha N, Puglisi A, Leuzzi L and Conti C 2013 *Scientific Rep.* **3** 2251
- [28] Ghofraniha N, Viola I, Di Maria F, Barbarella G, Gigli G, Leuzzi L and Conti C 2014 *Nat. Commun.* **6** 6058
- [29] Gomes A S L, Lima B C, Pincheira P I R, Moura A, Gagne M, Raposo E, de Araújo C B and Kashyap R 2016 *Phys. Rev. A* **94** 011801
- [30] Basak S, Blanco A and Lopez C 2016 *Sci. Rep.* **6** 32134
- [31] Pincheira P I R, Silva A F, Fewo S I and *et al* 2016 *Opt. Lett.* **41** 3459–3462
- [32] Gomes A S, Moura A L, de Araújo C B and Raposo E P 2021 *Progress in Quantum Electronics* **78** 100343 ISSN 0079-6727
- [33] Franzosi R, Livi R, Oppo G L and Politi A 2011 *Nonlinearity* **24** R89–R122 ISSN 0951-7715
- [34] Rasmussen K O, Cretigny T, Kevrekidis P G and Grønbech-Jensen N 2000 *Phys. Rev. Lett.* **84**(17) 3740–3743
- [35] Iubini S, Franzosi R, Livi R, Oppo G L and Politi A 2013 *New Journal of Physics* **15** 023032
- [36] Antenucci F, Crisanti A and Leuzzi L 2015 *Phys. Rev. A* **91** 053816
- [37] Skipetrov S and Sokolov I 2014 *Phys. Rev. Lett.* **112** 023905
- [38] Sperling T, Schertel L, Ackermann M, Aubry G J, Aegerter C M and Maret G 2016 *New J. Phys.* **18** 013039
- [39] Majumdar S N, Evans M R and Zia R K P 2005 *Phys. Rev. Lett.* **94**(18) 180601
- [40] Evans M R, Majumdar S N and Zia R K P 2006 *J. Stat. Phys.* **123** 357?–390
- [41] Trombettoni A and Smerzi A 2001 *Phys. Rev. Lett.* **86**(11) 2353–2356
- [42] Kevrekidis P 2009 *The Discrete Nonlinear Schroedinger Equation* (Springer Verlag (Berlin))
- [43] Livi R, Franzosi R and Oppo G L 2006 *Phys. Rev. Lett.* **97**(6) 060401
- [44] Iubini S and Politi A 2021 *Chaos, Solitons & Fractals* **147** 110954 ISSN 0960-0779
- [45] G Gotti S Iubini P P 2021 *Physical Review E* **103**

- [46] dynamics of a breather induced by an adiabatic invariant F 2022 *Journal of Statistical Mechanics: Theory and Experiment* 043206
- [47] Iubini S, Politi A and Politi P 2014 *J Stat Phys* **154** 1057–1073
- [48] S Iubini S Lepri A P 2012 *Physical Review E* **86** 011108
- [49] Iubini S, Lepri S, Livi R, Oppo G L and Politi A 2017 *Entropy* **19** 445
- [50] Antenucci F 2016 *Statistical physics of wave interactions* (Springer)
- [51] Antenucci F, Crisanti A, nez Berganza M I, Marruzzo A and Leuzzi L 2016 *Philosophical Magazine* **96** 704–731
- [52] Niedda J, Gradenigo G, Leuzzi L and Parisi G 2022 *arXiv:2210.04362*
- [53] Conti C and Leuzzi L 2011 *Phys. Rev. B* **83** 134204
- [54] Marruzzo A, Tyagi P, Antenucci F, Pagnani A and Leuzzi L 2018 *SciPost Phys.* **5** 002
- [55] Huang K 1987 *Statistical mechanics* (John Wiley & Sons)
- [56] Wiersma D S and Cavalieri S 2001 *Nature* **414** 708
- [57] Zhai T, Zhou Y, Chen S, Wang Z, Shi J, Liu D and Zhang X 2010 *Phys. Rev. A* **82**(2) 023824
- [58] Livi R, Pettini M, Ruffo S, Sparpaglione M and Vulpiani A 1985 *Phys. Rev. A* **31**(2) 1039–1045
- [59] Cretegnny T, Dauxois T, Ruffo S and Torcini A 1998 *Physica D: Nonlinear Phenomena* **121** 109–126
ISSN 0167-2789
- [60] Mujumdar S, Turck V, Torre R and Wiersma D S 2007 *Phys Rev A* **76** 033807
- [61] Hukushima K and Nemoto K 1996 *J. Phys. Soc. Japan* **65** 1604–1608